Structures and Electrocommunication between Ferrocenyl Groups in Osmium Cluster Complexes of 1,8-Bis(ferrocenyl)octatetrayne

Richard D. Adams,* O-Sung Kwon, Bo Qu, and Mark D. Smith

Department of Chemistry and Biochemistry and The USC NanoCenter, University of South Carolina, Columbia, South Carolina 29208

Received May 11, 2001

The reaction of $Os_3(CO)_{11}(NCMe)$, **1**, with 1,8-bis(ferrocenyl)octatetrayne, **3**, has yielded four new products: $Os_3(CO)_{10}(\mu_3\text{-}\eta^2\text{-Fc-C}_2\text{−C≡C−C≡C−C≡C−Fc})$, **4**; $Os_3(CO)_{10}(\mu_3\text{-}\eta^2\text{-Fc-C≡C−C}_2\text{−C≡C−C≡C−Fc})$, **5**; $Os_3(CO)_{11}(\mu_3\text{-}\eta^4\text{-Fc-C}_4\text{−C≡C−C≡C−Fc})$, **6**; and $Os_6(CO)_{21}(\text{Fc-C}_2\text{−C}_3\text{−COC−C≡C−Fc})$, **7**. Compounds **4** and **5** were obtained in better yields from the reaction of $Os_3(CO)_{10}(NCMe)_2$, **2**, with **3**, which also yielded a new hexaosmium compound, $Os_6(CO)_{20}(\mu_6\text{-}\eta^4\text{-Fc-C≡C−C}_2\text{−C≡C−C}_2\text{−Fc})$, **8**, formed by the addition of 2 equiv of **2** to **3**. All five products were characterized by IR, ^{1}H NMR, and single-crystal X-ray diffraction analysis. Compounds **4** and **5** are isomers containing a triply bridging bis(ferrocenyl)-octatetrayne ligand coordinated to a triangular triosmium cluster via different alkyne groups along the tetrayne chain. Compound **6** contains an open triosmium cluster coordinated in a parallel fashion to two adjacent triple bonds of the tetrayne chain of **3**. Compound **7** contains two triosmium clusters. One is open and the other is a closed triangle. A CO ligand was coupled to the tetrayne to form a five-membered heterocycle and a ferrocenyl carbocation along the C_8-chain. Compound **8** crystallized in two modifications. In both forms the molecular structure contains two closed triosmium clusters with triply bridging alkyne units coordinated to each cluster from the first and third alkyne groups of the tetrayne chain of **3**. In one crystal form each cluster has a bridging CO ligand. In the other modification there are no bridging CO ligands. The redox potentials of the ferrocenyl groups in **4**, **5**, and **8** are very the closely spaced, $\Delta E_p = 0.05$ V, $\Delta E_p = 0.02$ V, and $\Delta E_p = 0.03$ V, respectively, suggesting that there is very little electrocommunication between them, but compound **6** shows two resolved one-electron redox processes, $\Delta E_p = 0.14$ V, indicating that there may be significant electrocommunication in this case. This is attributed to greater interactions in the π-orbtial network in the ligand **3** induced by coordination to the metal atoms.

Introduction

There is much interest in trying to utilize polyunsaturated hydrocarbons as "molecular" wires for the construction of nanoscale electronic devices.[1,2] Electronic communication through such potential molecular wires is often evaluated by examining the redox response of electroactive groups placed at their terminii.[2] We have recently shown that the attachment of osmium carbonyl clusters to 1,4-bis(ferrocenyl)butadiyne can lead to enhancement of the electrocommunication through the butadiyne chain when the osmium atoms are coordinated parallel to the chain, as found in the compound $Os_3(CO)_{11}(\mu_3\text{-}\eta^4\text{-FcCCCCFc})$, **A**, Fc = $C_5H_4FeC_5H_5$, and leads to a decrease in the electrocommunication when the osmium atoms are coordinated as a triangle to both π-bonds of a single C−C triple bond, as found in $Os_3(CO)_{10}(\mu_3\text{-}\eta^2\text{-FcCCCCFc})$, **B**.[3] This has been attributed to differing effects of the metal atoms on the π-bonding along the C_4 diyne chain.[3]

To try to study this phenomenon further, we have now investigated the coordination of 1,8-bis(ferrocenyl)-octatetrayne to triosmium cluster complexes. Our studies of the reactions of $Os_3(CO)_{11}(NCMe)$, **1**, and $Os_3(CO)_{10}(NCMe)_2$, **2**, with 1,8-bis(ferrocenyl)octatetrayne, **3**, have yielded three new products containing a trios-

* Corresponding author. E-mail: Adams@mail.chem.sc.edu.

(1) *Molecular Electronics: Science and Technology*, Aviram, A., Ed.; Confer. Proc. No. 262, American Institute of Physics: New York, 1992. (b) *Molecular and Biomolecular Electronics*, Birge, R. R., Ed.; Advances in Chemistry Series 240; American Chemical Society, 1991. (c) *Nanostructures and Mesoscopic Systems*; Kirk, W. P., Reed, M. A., Eds.; Academic: New York, 1992. (d) Astruc, D. *Electron Transfer and Radical Processes in Transition-Metal Chemistry*; VCH Publishers: New York, 1995; Chapter 4. (e) Collier, C. P.; Wong, E. W.; Belohradsky, M.; Raymo, F. M.; Stoddart, J. F.; Kuekes, P. J.; Williams, R. S.; Heath, J. R. *Science* **1999**, *285*, 391. (f) Feldheim, D.; Keating, C. D. *Chem. Soc. Rev.* **1998**, *27*, 1. (g) Andres, R. P.; Bielefeld, J. D.; Henderson, J. I.; Janes, D. B.; Kolagunta, V. R.; Kubiak, C. P.; Mahoney, W. J.; Osifchin, R. G. *Science* **1996**, *273*, 1690.

(2) Paul, F.; Lapinte, C. *Coord. Chem. Rev.* **1998**, *178−180*, 431. (b) Ward, M. D. *Chem. Soc. Rev.* **1995**, 121. (c) Barlow, S.; O'Hare, D. *Chem. Rev.* **1997**, *97*, 637. (d) Grosshenny, V.; Harriman, A.; Hissler, M.; Ziessel, R. *Plat. Met. Rev.* **1996**, *40*, 26. (e) Grosshenny, V.; Harriman, A.; Hissler, M.; Ziessel, R. *Plat. Met. Rev.* **1996**, *40*, 72. (f) Kheradmandan, S.; Heinze, K.; Schmalle, H. W.; Berke, H. *Angew. Chem., Int. Ed.* **1999**, *38*, 2270. (g) Tarraga, A.; Molina, P.; Curiel, D.; Desamparados Velasco, M. *Organometallics* **2001**, *20*, 2145.

(3) Adams, R. D.; Qu, B. *Organometallics* **2000**, *19*, 2411.

10.1021/om0104060 CCC: $20.00
Publication on Web 10/26/2001

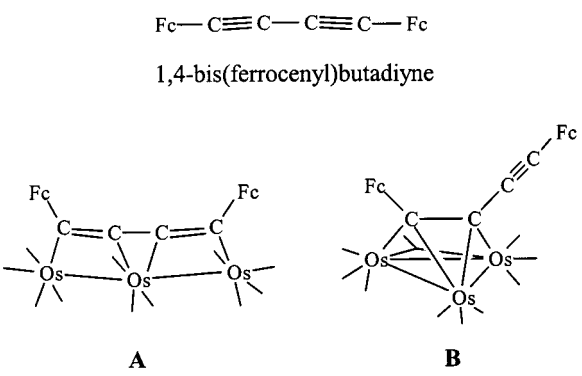

mium cluster and two new products containing two triosmium clusters. All five compounds have been characterized crystallographically and by electrochemical methods. These results are reported here.

Experimental Section

General Data. All the reactions were performed under an atmosphere of nitrogen. Reagent grade solvents were dried and freshly distilled prior to use. $Os_3(CO)_{11}(NCMe)$,[4] **1**, $Os_3(CO)_{10}(NCMe)_2$,[4] **2**, and 1,8-bis(ferrocenyl)octatetryne,[5] **3**, were prepared according to literature procedures. Product separations was performed by TLC in air on Analtech 0.25 mm silica gel 60 Å F_{254} glass plates. Infrared spectra were recorded on a Nicolet 5 DXB FT-IR spectrophotometer. ^{1}H NMR spectra were run on a Bruker AM-300 spectrometer operating at 300 MHz. Elemental analyses were performed by Desert Analytics, Tucson, AZ. Electronic absorption spectra were recorded with a Perkin-Elmer Lambda 14 UV−visible spectrophotometer in methylene chloride solvent.

Reaction of 1 with 3. A 25 mg amount of **1** (0.0272 mmol) and a 12.7 mg amount of **3** (0.0272 mmol) were dissolved in 30 mL of CH_2Cl_2 in a 100 mL three-necked round-bottomed flask. The solution was stirred at 25 °C for 1 h. The solvent was then removed in vacuo, and the residue was dissolved in a minimal amount of CH_2Cl_2 and separated by TLC on silica gel by using a hexane/CH_2Cl_2 (3:1) solvent mixture to yield in order of elution 2.6 mg of unreacted **3**; 0.5 mg of orange $Os_3(CO)_{10}(\mu_3\text{-}\eta^2\text{-Fc-}C_2\text{−}C\equiv C\text{−}C\equiv C\text{−}C\equiv C\text{−Fc})$, **4** (1% yield); 2.0 mg of red $Os_3(CO)_{10}(\mu_3\text{-}\eta^2\text{-Fc-}C\equiv C\text{−}C_2\text{−}C\equiv C\text{−}C\equiv C\text{−Fc})$, **5** (6% yield); 10.3 mg of red $Os_3(CO)_{11}(\mu_3\text{-}\eta^4\text{-Fc-}C_4\text{−}C\equiv C\text{−}C\equiv C\text{−Fc})$, **6** (28% yield); and 1.2 mg of $Os_6(CO)_{21}(\text{Fc-}C_2\text{−}C_3\text{−COC−}C\equiv C\text{−Fc})$, **7** (2% yield). Analytical and spectral data for **4**: IR ν_{CO} (cm^{-1} in hexane): 2100 (m), 2069 (vs), 2056 (s), 2031 (m), 2016 (w), 2009 (m), 1982 (w), 1845 (w). ^{1}H NMR (δ in $CDCl_3$): 4.25 (s, 5H, Cp), 4.25 (m, 1H, C_5H_4), 4.27 (s, 5H, Cp), 4.27 (m, 1H, C_5H_4), 4.36 (m, 2H, C_5H_4), 4.52−4.55 (m, 4H, C_5H_4). Anal. Calcd (found): C 34.66 (34.59); H 1.37 (1.40). For **5**: IR ν_{CO} (cm^{-1} in hexane): 2102 (m), 2069 (vs), 2064 (vs, sh), 2031 (s), 2010 (m), 1850 (vw). ^{1}H NMR (δ in $CDCl_3$): 4.17 (s, 5H, Cp), 4.22−4.23 (m, 4H, $2C_5H_4$), 4.40−4.41 (m, 2H, C_5H_4), 4.43−4.44 (m, 2H, C_5H_4), 4.22 (s, 5H, Cp). Anal. Calcd (found): C 34.66 (35.09); H 1.37 (1.44). For **6**: IR ν_{CO} (cm^{-1} in hexane): 2127 (m), 2100 (s), 2045 (vs), 2014 (m), 2003 (m), 1972 (m), 1961 (m). ^{1}H NMR (δ in $CDCl_3$): 4.16 (s, 5H, Cp), 4.26 (s, 5H, Cp), 4.27 (m, 2H, C_5H_4), 4.49 (m, 2H, C_5H_4), 4.53 (m, 2H, C_5H_4), 4.57 (m, 2H, C_5H_4). Anal. Calcd (found): C 34.83 (35.43); H 1.34 (1.65). For **7**: IR ν_{CO} (cm^{-1} in hexane): 2126 (w), 2105 (m), 2081 (s), 2056 (vs), 2048 (vs), 2042 (vs), 2010 (s), 1985 (w), 1973 (m), 1965 (m), 1857 (w). ^{1}H NMR (δ in $CDCl_3$): 4.20 (s, 5H, Cp), 4.19(m, 1H, C_5H_4), 4.23 (m, 1H, C_5H_4), 4.34−4.38 (m, 2H, C_5H_4), 4.56 (m, 1H, C_5H_4). 4.57 (s, 5H, Cp), 4.75 (m, 1H, C_5H_4), 5.05 (m, 1H, C_5H_4), 5.14 (m, 1H, C_5H_4), UV−vis: λ_{max} = 544 nm, ϵ = 18 500 M^{-1} cm^{-1}; λ_{max} = 625 nm, ϵ = 18 500 M^{-1} cm^{-1}. Anal. Calcd (found): C 27.01 (28.18); H 0.81 (0.89).

Reaction of 2 with 3. A 30.0 mg amount of **2** (0.0322 mmol) and a 15.0 mg amount of **3** (0.0322 mmol) were dissolved in 30 mL of hexane in a 100 mL three-necked round-bottomed flask. The solution was heated to reflux for 30 min. The solvent was then removed in vacuo, and the residue was dissolved in a minimal amount of CH_2Cl_2 and separated by TLC on silica gel with a hexane/CH_2Cl_2 (3:1) solvent mixture to yield in order of elution 3.2 mg of unreacted **3**; 2.1 mg of **4**, 5% yield; 22.8 mg of **5**, 54% yield; and 8.2 mg of red orange $Os_6(CO)_{20}(\mu_6\text{-}\eta^4\text{-Fc-}C\equiv C\text{−}C_2\text{−}C\equiv C\text{−}C_2\text{−Fc})$, **8**, in a 12% yield. Analytical and spectral data for **8**: IR ν_{CO} (cm^{-1} in hexane): 2103 (w), 2096 (m), 2070 (vs), 2053 (m), 2030 (m), 2008 (m), 1845 (vw). ^{1}H NMR (δ in $CDCl_3$): 4.11 (s, 5H, Cp), 4.20 (m, 2H, C_5H_4), 4.23 (m, 2H, C_5H_4), 4.26 (s, 5H, Cp), 4.31 (m, 2H, C_5H_4). 4.65 (m, 2H, C_5H_4). Anal. Calcd (found): C 26.60 (26.53); H 0.83 (0.66).

Synthesis of 7 from 6 and 1. A 10 mg amount of **6** (0.00744 mmol) and a 13.7 mg amount of **1** (0.0149 mmol) were dissolved in 25 mL of CH_2Cl_2 in a 50 mL round-bottomed flask and stirred at 25 °C for 5 h. The solvent was then removed in vacuo. The product **7** was isolated by TLC on silica gel by using a hexane/CH_2Cl_2 (3:1) solvent mixture to give 3.5 mg, 22% yield.

Synthesis of 8 from 5 and 2. A 17 mg amount of **5** (0.01291 mmol) and a 13 mg amount of **2** (0.01394 mmol) were dissolved in 25 mL of hexane in a 50 mL three-necked round-bottom flask. The resulting solution was heated to reflux for 25 min. The solvent was then removed by rotoevaporation. The product **8** was isolated by TLC on silica gel by using a hexane/CH_2Cl_2 (3:1) solvent mixture to give 23.8 mg, 85% yield.

Crystallographic Analyses. Red crystals of **4** were grown by slow evaporation of the solvent from CH_2Cl_2/hexane (1:6) solution of the complex at −20 °C. Dark red crystals of **5** were grown by slow evaporation of the solvent from ethyl ether solution of the complex at −20 °C. Dark red crystals of **6** were grown by slow evaporation of the solvent from hexane/CH_2Cl_2 (4:1) solution of the complex at 25 °C. Dark red crystals of **7** were grown by slow evaporation of the solvent from benzene/CH_2Cl_2 (2:1) solution of the complex at 25 °C. Red crystals of **8** were grown by slow evaporation of the solvent from a benzene/octane (1:1) solution of the complex at 25 °C.

The crystals of **4**, **5**, **6**, **7**, and **8** used in data collections were each glued onto the end of thin glass fibers. X-ray intensity data were measured at 293 K on a Bruker SMART APEX CCD-based diffractometer using Mo Kα radiation (λ = 0.71073 Å). Compound **5** was measured at 193 K. The unit cells were determined based on reflections collected from a set of three frames measured in orthogonal wedges of reciprocal space. Crystal data, data collection parameters, and results of the analyses are listed in Tables 1 and 2. The raw intensity data frames were integrated with the SAINT+ program using a narrow-frame integration algorithm.[6] Corrections for Lorentz and polarization effects were also applied by SAINT. For each analysis an empirical absorption correction based on the multiple measurement of equivalent reflections was applied by using the program SADABS.[6]

Compounds **4** and **5** crystallized in the monoclinic crystal system. The space group *C*2/*c* was indicated by the systematic absences and confirmed by the successful solution and refinement of the structure. Compound **6** crystallized in the monoclinic crystal system. The space group $P2_1/c$ was confirmed by the systematic absences in the data. Compound **7** crystallized in the triclinic crystal system. The space group *P*1 was assumed and confirmed by the successful solution and refinement of the structure.

(4) Drake, S. R.; Khattar, R. *Organomet. Synth.* **1988**, *4*, 234.
(5) Yuan, Z.; Stringer, G.; Jobe, I. R.; Kreller, D.; Scott, K.; Koch, L.; Taylor, N. J.; Marder, T. B. *J. Organomet. Chem.* **1993**, *452*, 115.
(6) *SAINT*+ Version 6.02a; Bruker Analytical X-ray System, Inc.: Madison, WI, 1998.

Table 1. Crystallographic Data for Compounds 4−6

	4	5	6
empirical formula	$Os_3Fe_2O_{10}C_{38}H_{18}\cdot 1/2C_6H_{14}$	$Os_3Fe_2O_{10}C_{38}H_{18}\cdot 1/2\ C_4H_{10}O$	$Os_3Fe_2O_{11}C_{39}H_{18}$
fw	1359.91	1353.88	1344.83
cryst syst	monoclinic	monoclinic	monoclinic
lattice params			
a (Å)	17.6758(9)	40.129(3)	20.7688(11)
b (Å)	9.5825(5)	7.4272(6)	10.7666(6)
c (Å)	47.558(3)	24.917(2)	17.8136(9)
α (deg)	90	90	90
β (deg)	90.947 (1)	95.585 (2)	109.677(1)
γ (deg)	90	90	90
V (Å^3)	8044.7 (7)	7688 (1)	3750.7 (3)
space group	*C*2/*c* (#15)	*C*2/*c* (#15)	$P2_1/c$ (#14)
Z value	8	8	4
ρ_{calc} (g/cm^3)	2.246	2.339	2.382
μ (Mo Kα) (mm^{-1})	11.202	10.676	10.942
temperature (K)	293	173	293
$2\theta_{max}$ (deg)	52.76	52.80	52.80
no. of obsd reflns ($I > 2\sigma(I)$)	4246	5998	5277
no. of params	436	487	496
goodness of fit	0.982	1.035	0.962
max. shift in cycle	0.028	0.001	0.005
residuals: R1; wR2	0.0542; 0.0967	0.0386; 0.0742	0.0352; 0.0720
abs corr, max/min	SADABS, 0.491; 0.321	SADABS, 0.745; 0.337	SADABS, 0.647; 0.292
largest peak in final diff map (e$^-$/Å^3)	2.630	1.999	2.208

Table 2. Crystallographic Data for Compounds 7, 8a, and 8b

	7	8a	8b
empirical formula	$Os_6Fe_2O_{22}C_{50}H_{18}$	$Os_6Fe_2O_{20}C_{48}H_{18}$	$Os_6Fe_2O_{20}C_{48}H_{18}$
fw	2223.45	2167.52	2167.52
cryst syst	triclinic	monoclinic	triclinic
lattice params			
a (Å)	10.1980(5)	11.8144(9)	9.4725(9)
b (Å)	23.0028(12)	27.836(2)	13.7168(13)
c (Å)	25.9432(13)	15.867(1)	21.624(2)
α (deg)	96.331(1)	90	102.827(2)
β (deg)	96.951(1)	98.756(2)	95.057(2)
γ (deg)	97.097(1)	90	99.309(2)
V (Å^3)	2973.1(2)	5157.4(7)	2680.8(4)
space group	$P\bar{1}$ (#2)	$P2_1/n$ (#14)	$P\bar{1}$ (#2)
Z value	2	4	2
ρ_{calc} (g/cm^3)	2.484	2.792	2.685
μ(Mo Kα) (mm^{-1})	13.312	15.341	14.756
temperature (K)	293	293	293
$2\theta_{max}$ (deg)	50.04	50.16	50.22
no. of obsd reflns ($I > 2\sigma(I)$)	11 733	6612	5630
no. of params	1409	685	685
goodness of fit	1.004	1.018	1.008
max. shift in cycle	0.001	0.007	0.001
residuals: R1; wR2	0.0568; 0.123	0.0345; 0.0714	0.0547; 0.1016
abs corr, max/min	SADABS 0.825; 0.087	SADABS 0.193; 0.078	SADABS 0.694; 0.561
largest peak in final diff map (e$^-$/Å^3)	2.966	1.990	1.816

Compound **8** crystallized in the monoclinic crystal system. The space group $P2_1/n$ was confirmed by the systematic absences in the intensity data. A second crystallographic modification of **8** cocrystallized from the solutions in the triclinic crystal system. The space group $P\bar{1}$ was assumed and confirmed by the successful solution and refinement of the structure. The structures of **4**, **5**, **6**, **7**, and both polymorphs of **8** were solved by a combination of direct methods and difference Fourier syntheses and refined by full-matrix least-squares on F^2, using the SHELXTL software.[7] All non-hydrogen atoms were refined with anisotropic displacement parameters. The positions of the hydrogen atoms were calculated by assuming idealized geometries and were included in the structure factor calculation without refinement.

Electrochemical Measurements. Cyclic and differential pulse voltammetric measurements (DPV) were performed by using a three-electrode system consisting of a glassy carbon working electrode, a platinum counter electrode, and a Ag/AgCl reference electrode on a CV-50W voltammetric analyzer purchased from Bioanalytical Systems, West Lafayette, IN. Samples were prepared in 1.0 mM solutions by using a CH_2Cl_2/CH_3CN (1:1) solvent mixture containing 0.1 M tetrabutylammonium hexafluorophosphate. The DP voltammogram of compound **4** shows two closely spaced one-electron oxidations for the ferrocenyl groups at $E = +0.50$ V and $+0.55$ V vs Ag/AgCl, $\Delta E_p = 0.05$ V. The DP voltammogram of compound **5** exhibits two very closely spaced and poorly resolved one-electron oxidations for the ferrocenyl groups at $E = +0.49$ V and $+0.51$ V (shoulder) vs Ag/AgCl, $\Delta E_p = 0.02$ V. The DP voltammogram of compound **6** shows two resolved one-electron oxidations for the ferrocenyl groups at $E = +0.38$ V and $+0.52$ V vs Ag/AgCl, $\Delta E_p = 0.14$ V. Compound **7** shows two only poorly resolved irreversible oxidations. Compound **8** shows two very closely spaced, poorly resolved one-electron oxidations for the ferrocenyl groups at $E = +0.47$ V (shoulder) and $+0.50$ V vs Ag/AgCl, $\Delta E_p = 0.03$ V. The cyclic voltammo-

(7) Sheldrick, G. M. *SHELXTL* Version 5.1; Bruker Analytical X-ray Systems, Inc.: Madison, WI, 1997.

Scheme 1

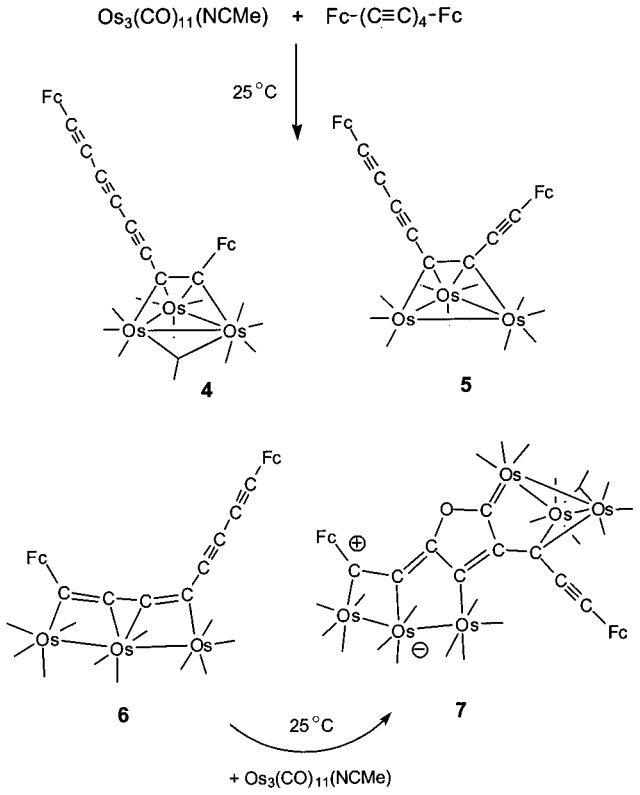

grams of **4**, **5**, **6**, and **8** showed that these redox processes were reversible.

Results

The reaction of $Os_3(CO)_{11}(NCMe)$, **1**, with 1,8-bis(ferrocenyl)octatetrayne, **3**, has yielded four new products: $Os_3(CO)_{10}(\mu_3\text{-}\eta^2\text{-Fc-}C_2\text{-}C{\equiv}C\text{-}C{\equiv}C\text{-}C{\equiv}C\text{-Fc})$, **4**; $Os_3(CO)_{10}(\mu_3\text{-}\eta^2\text{-Fc-}C{\equiv}C\text{-}C_2\text{-}C{\equiv}C\text{-}C{\equiv}C\text{-Fc})$, **5**; $Os_3(CO)_{11}(\mu_3\text{-}\eta^4\text{-Fc-}C_4\text{-}C{\equiv}C\text{-}C{\equiv}C\text{-Fc})$, **6**; and $Os_6(CO)_{21}(\text{Fc-}C_2\text{-}C_3\text{-}COC\text{-}C{\equiv}C\text{-Fc})$, **7**, as shown in Scheme 1. The yields of **4**, **5**, and **7** were low: 1%, 6%, and 2%, respectively. Compound **6** is the major product at 28% yield. The yields of **4** and **5** were subsequently improved to 5% and 54%, respectively, in the reaction of **2** with **3**. Compounds **4**−**6** were characterized by IR, ^{1}H NMR, and single-crystal X-ray diffraction analysis and by differential pulse voltammetry (DPV). ORTEP diagrams of the molecular structures of **4** and **5** are shown in Figures 1 and 2, respectively. Selected interatomic distances and angles are listed in Table 3. Compounds **4** and **5** are isomers. Both contain compound **3** as a ligand coordinated to the cluster through one of its C−C triple bonds. In **4** the ligand is coordinated through one of the outer C−C triple bonds. In **5** it is coordinated through one of the two "inner" triple bonds of **3**. In both compounds the coordinated alkyne group has adopted the μ_3-|| mode that is commonly observed for alkynes coordinated in 48 e$^-$ clusters.[8] The coordinated C−C triple bond has increased in length as a result of the coordination: C(1)−C(2) in **4** equals 1.450(16) Å, C(3)−C(4) in **5** equals 1.435(12) Å. These values are

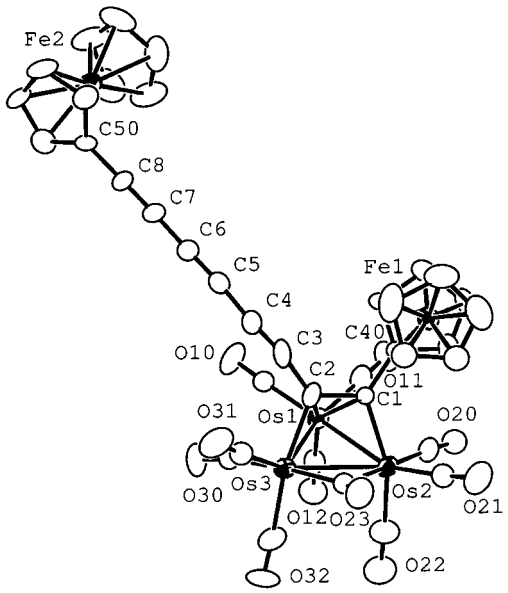

Figure 1. ORTEP diagram of $Os_3(CO)_{10}(\mu_3\text{-}\eta^2\text{-Fc-}C_2\text{-}C{\equiv}C\text{-}C{\equiv}C\text{-}C{\equiv}C\text{-Fc})$, **4**, showing 40% probability thermal ellipsoids.

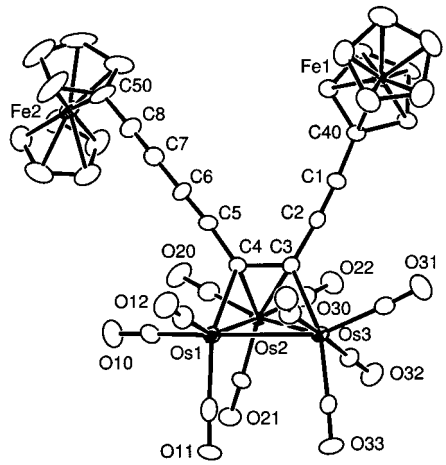

Figure 2. ORTEP diagram of $Os_3(CO)_{10}(\mu_3\text{-}\eta^2\text{-Fc}{-}C{\equiv}C{-}C_2{-}C{\equiv}C{-}C{\equiv}C{-}\text{Fc})$, **5**, showing 40% probability thermal ellipsoids.

typical of alkynes coordinated in the μ_3-|| mode[8] and are similar to the coordinated C−C triple bond distance of 1.40(2) Å observed in compound **B**.[3] The uncoordinated C−C triple bonds in both molecules are characteristically short, ranging from 1.174(12) to 1.206(12) Å. Both compounds contain closed triangular triosmium clusters with 10 carbonyl ligands. In compound **4** nine of the CO ligands are terminal and one, C(23)−O(23), is a bridging ligand. In compound **5** nine of the CO ligands are terminal, but the tenth, C(30)−O(30), is a semibridging CO ligand. We were unable to interconvert **4** and **5** by thermal treatment at 125 °C.

Compound **6** contains an open triosmium cluster with 11 terminal carbonyl ligands. The three metal atoms are coordinated to two adjacent alkyne units, C(1)−C(2) and C(3)−C(4), in a linear mode parallel to the C−C bonds. These coordinated triple bonds are also lengthened as a result of the coordination: C(1)−C(2) = 1.333(9) Å and C(3)−C(4) = 1.317(9) Å, but not as much as that observed for the coordinated triply bridging C−C

(8) Deabate, S.; Giordano, R.; Sappa, E. *J. Cluster Sci.* **1997**, *8*, 407. (b) Deeming, A. J. *Adv. Organomet. Chem.* **1986**, *26*, 1. (c) Raithby, P. R.; Rosales, M. *Adv. Inorg. Radiochem.* **1985**, *29*, 169.

Table 3. Selected Bond Lengths (Å) and Angles (deg) for Compounds 4−6[a]

	4	5	6
	Distances		
Os1−Os2	2.7577(8)	2.7267(5)	2.9431(4)
Os2−Os3	2.8331(8)	2.8220(6)	2.9346(4)
Os1−Os3	2.7835(8)	2.8635(5)	
Os1−C1	2.328(12)		2.133(8)
Os2−C1	2.067(14)		
Os1−C2	2.244(14)		
Os2−C2			2.273(7)
Os3−C2	2.128(18)		
Os1−C4		2.096(9)	
Os2−C4		2.257(8)	
Os3−C4			2.150(7)
Os2−C3		2.233(8)	2.302(8)
Os3−C3		2.133(9)	
C1−C2	1.450(16)	1.174(12)	1.333(9)
C2−C3	1.42(3)	1.450(13)	1.305(9)
C3−C4	1.19(2)	1.435(12)	1.317(9)
C4−C5	1.39(2)	1.445(12)	1.407(10)
C5−C6	1.20(2)	1.206(12)	1.200(10)
C6−C7	1.36(2)	1.374(14)	1.369(11)
C7−C8	1.20(2)	1.194(14)	1.192(11)
	Angles		
Os1−Os2−Os3	59.70(2)	62.111(14)	160.554(15)
Os2−Os1−Os3	61.50(2)	60.574(14)	
Os1−Os3−Os2	58.80(2)	57.311(13)	
C2−C1−C40	120.1(13)	175.3(10)	119.7(7)
C1−C2−C3	127.1(16)	173.9(9)	168.2(8)
C2−C3−C4	171(2)	120.7(8)	171.7(8)
C3−C4−C5	174.2(18)	121.1(8)	121.7(7)
C4−C5−C6	173.7(19)	171.9(9)	176.8(8)
C5−C6−C7	178.3(18)	178.1(11)	175.7(8)
C6−C7−C8	177.7(18)	176.2(11)	175.8(9)
C7−C8−C50	180(2)	178.6(13)	174.2(9)

[a] Estimated standard deviations given in parentheses.

bonds in **4** and **5**. Interestingly, the C−C distance between the two triple bonds has decreased in length, C(2)−C(3) = 1.305(9) Å. This will be explained below. The coordination of **3** to the osmium cluster in **6** is similar to that observed for the coordination of 1,4-bis-(ferrocenyl)butadiyne to the open triosmium cluster in $Os_3(CO)_{11}(\mu_3\text{-}\eta^4\text{-FcCCCCFc})$, **A**, where a similar shortening of the C−C bond length between the two coordinated C−C triplc bonds was also observed.[3] The uncoordinated C−C bonds of the tetrayne grouping exhibit normal bonding distances, C(5)−C(6) = 1.200(10) Å, C(6)−C(7) = 1.369(11) Å, and C(7)−C(8) = 1.191(11) Å.

Compound **7** was also obtained independently in 22% yield from the reaction of **6** with **1**. Compound **8** was also obtained independently in 85% yield from the reaction of **5** with **2**. Compounds **7** and **8** were both characterized crystallographically. Compounds **7** and **8** both contain six osmium atoms arranged into two triosmium clusters. Selected interatomic distances and angles for **7** and **8** are listed in Table 4. An ORTEP diagram of the molecular structure of **7** is shown in Figure 4. The cluster Os(1)−Os(3) is open and contains 11 carbonyl ligands and is similar to the triosmium cluster found in **6**. Cluster Os(4)−Os(6) contains 10 carbonyl ligands and is triangular with three metal−metal bonds. Interestingly, compound **7** contains a five-membered heterocycle that formed along the C_8-chain of the original tetrayne grouping by the coupling of a CO ligand to two of the carbon atoms, C(3) and C(5). The formation of the heterocycle significantly alters the bonding along the tetrayne chain. We favor the

Table 4. Selected Bond Lengths (Å) and Angles (deg) for Compounds 7, 8a, and 8b[a]

	7	8a	8b
	Distances		
Os1−Os2	2.8391(12)	2.7323(6)	2.8575(11)
Os2−Os3	2.8954(11)	2.8665(6)	2.8855(11)
Os1−Os3		2.7996(6)	2.7046(12)
Os4−Os5	2.8321(10)	2.8363(6)	2.7133(10)
Os5−Os6	2.7677(10)	2.7745(6)	2.8353(11)
Os4−Os6	2.8637(11)	2.7394(6)	2.8697(10)
Os1−C1	2.120(17)		
Os2−C2	2.179(14)		
Os1−C4		2.214(9)	2.289(17)
Os3−C4	2.116(17)	2.166(9)	2.079(15)
Os1−C3		2.294(9)	2.153(17)
Os2−C3		2.072(8)	2.154(15)
Os5−C6	2.197(16)		
Os5−C7		2.127(9)	2.173(17)
Os6−C7	2.231(15)	2.198(9)	2.201(17)
Os6−C8		2.319(9)	
Os4−C8		2.079(9)	2.108(15)
Os5−C8			2.313(17)
Os4−C9	2.043(14)		
C1−C2	1.37(2)	1.190(13)	1.16(2)
C2−C3	1.33(2)	1.448(13)	1.46(2)
C3−C4	1.46(2)	1.410(12)	1.44(2)
C4−C5	1.41(2)	1.422(12)	1.42(2)
C5−C6	1.46(2)	1.196(12)	1.21(2)
C6−C7	1.42(2)	1.438(12)	1.40(2)
C7−C8	1.23(2)	1.413(12)	1.40(2)
C5−C9	1.40(2)		
C3−O9	1.42(2)		
C9−O9	1.35(2)		
	Angles		
Os1−Os2−Os3	149.46(3)	59.948(15)	56.19(3)
Os2−Os1−Os3		62.407(14)	62.43(3)
Os1−Os3−Os2		57.645(14)	61.38(3)
Os4−Os5−Os6	61.50(3)	58.436(15)	62.24(3)
Os4−Os6−Os5	60.36(3)	61.911(16)	56.79(2)
Os5−Os4−Os6	58.14(3)	59.653(15)	60.97(3)
C2−C1−C70	118.9(16)	174.9(11)	180(2)
C1−C2−C3	149.0(15)	174.5(10)	169.4(19)
C2−C3−C4	126.2(14)	121.6(8)	123.7(15)
C3−C4−C5	102.8(14)	125.2(8)	120.7(15)
C6−C5−C4	132.8(15)	175.4(10)	172.6(18)
C5−C6−C7	118.2(13)	175.0(10)	171.6(18)
C8−C7−C6	173.9(18)	126.4(8)	131.3(16)
C7−C8−C80	175(2)	122.9(8)	121.6(14)
C3−O9−C9	105.4(11)		
C5−C9−O9	111.4(12)		
C9−C5−C4	109.1(14)		
C4−C3−O9	110.5(14)		
C6−C5−C9	117.9(14)		

[a] Estimated standard deviation in the least significant figure is given in parentheses.

zwitterionic resonance structure shown in Scheme 1. Carbon C(1) is trivalent and nearly planar. The sum of the angles around C(1) equals 359°. This carbon atom is characteristic of ferrocenyl carbocations.[10] This is supported by the UV−vis absorption spectrum that will be described below. The Os(2)−C(1) distance of 2.594-(16) Å is believed to be largely nonbonding. The distance C(2)−C(3) at 1.33(2) Å is short and assigned as a double bond. The distance C(3)−C(4) at 1.45(2) Å is one of the longest and is formulated as a single bond. To satisfy valence, the C(4)−C(5) bond at 1.41(2) Å is assigned

(9) Watts, W. E. In *Comprehensive Organometallic Chemistry;* Wilkinson, G., Stone, F. G. A., Abel, E., Eds.; Pergamon Press: Oxford, 1982; Chapter 59, p 1052. (b) Watts, W. E. *Organomet. Chem. Rev.* **1979**, *7*, 399.

(10) Adams, R. D.; Chen, G. *Organometallics* **1990**, *9*, 2882. (b) Adams, R. D.; Chen, G. *Organometallics* **1991**, *10*, 3020. (c) Adams, R. D. *Chem. Rev.* **1989**, *89*, 1703.

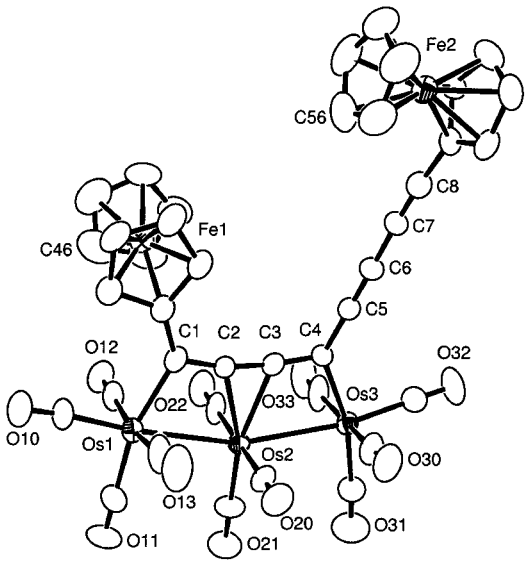

Figure 3. ORTEP diagram of $Os_3(CO)_{11}(\mu_3\text{-}\eta^4\text{-Fc-}C_2\text{-}C{\equiv}C\text{-}C{\equiv}C\text{-Fc})$, **6**, showing 40% probability thermal ellipsoids.

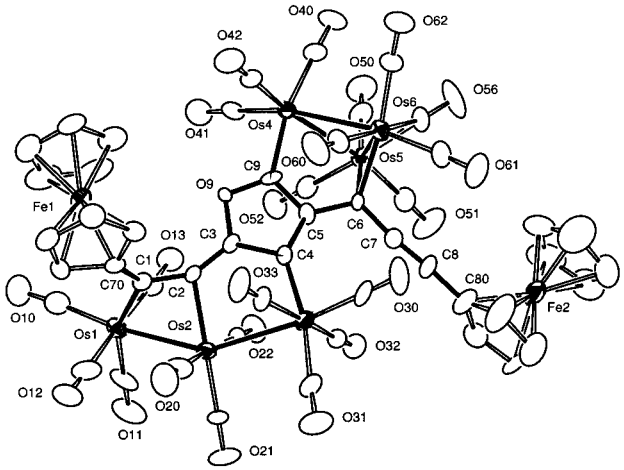

Figure 4. ORTEP diagram of $Os_6(CO)_{21}(Fc\text{-}C_2\text{-}C_3\text{-}COC\text{-}C{\equiv}C\text{-Fc})$, **7**, showing 40% probability thermal ellipsoids.

Scheme 2

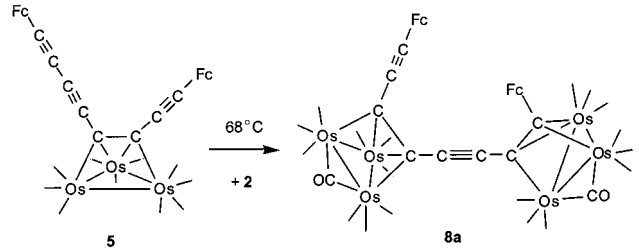

formally as a double bond. Atom C(9) is formulated as a carbene center, and the bond between Os(4) and C(9) is short, as expected for an Os−C double bond, 2.043(14) Å.[9] Atom C(6) is a carbene center that bridges the Os(5)−Os(6) bond in the triangular cluster. There is a C−C triple bond between atoms C(7)−C(8), 1.23(2) Å. The UV−vis spectrum of **7** exhibits two strong low-energy absorptions at $\lambda_{max} = 544$ nm, $\epsilon = 18\,500$ M^{-1} cm^{-1}; $\lambda_{max} = 625$ nm, $\epsilon = 18\,500$ M^{-1} cm^{-1}. These absorptions are characteristic of ferrocenyl carbocations.[11]

The reaction of the decacarbonyl cluster complex **2** with **3** provided **4** and **5** in much better yields, 5% and

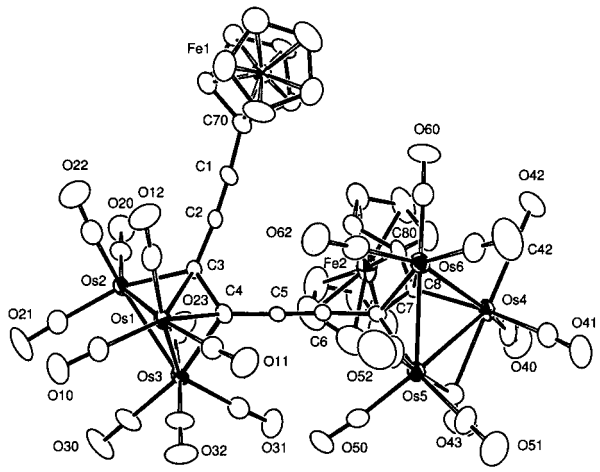

Figure 5. ORTEP diagram of $Os_6(CO)_{20}(\mu_6\text{-}\eta^4\text{-Fc}{-}C{\equiv}C{-}C_2{-}C{\equiv}C{-}C_2{-}Fc)$, **8a**, showing 40% probability thermal ellipsoids.

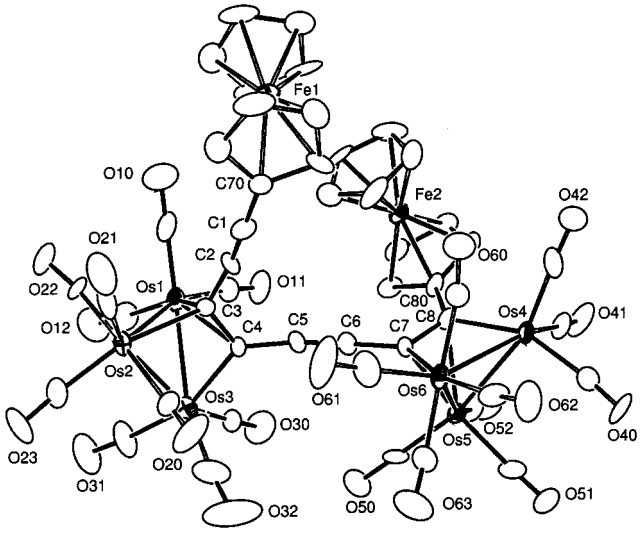

Figure 6. ORTEP diagram of $Os_6(CO)_{20}(\mu_6\text{-}\eta^4\text{-Fc}{-}C{\equiv}C{-}C_2{-}C{\equiv}C{-}C_2{-}Fc)$, **8b**, showing 40% probability thermal ellipsoids.

54%, respectively, and also the new hexaosmium compound $Os_6(CO)_{20}(\mu_6\text{-}\eta^4\text{-Fc-}C{\equiv}C{-}C_2{-}C{\equiv}C{-}C_2{-}Fc)$, **8**, in a 12% yield. Note, the yield of **5** is again much larger than that of **4**. In addition, compound **8** was prepared in a good yield (85%) from the reaction of **5** with **2**; see Scheme 2. Compound **8** crystallizes in two modifications: a monoclinic form **8a** and a triclinic from **8b**. ORTEP diagrams of the molecular structures of **8a** and **8b** are shown in Figures 5 and 6, respectively. The analyses show that **8a** and **8b** are isomers. In both structures the molecule contains two closed triangular clusters with a triply bridging alkyne unit, one inner and one outer position of the tetrayne chain, on the face of each triangle. The major difference between the molecular structures is the arrangement of the CO ligands on the osmium clusters. In **8a** both osmium clusters contain nine terminal CO ligands and one bridging CO ligand, while in **8b** the osmium clusters both have 10 terminal CO ligands. In addition, the

(11) Lukasser, J.; Angleitner, H.; Schottenberger, H.; Kopacka, H.; Schweiger, M.; Bildstein, B.; Ongania, K.-H.; Wurst, K. *Organometallics* **1995**, *14*, 5566. (b) Ansorge, M.; Polborn, K.; Müller, T. J. J. *Eur. J. Inorg. Chem.* **2000**, 2003.

structures also exhibit slightly different conformations when viewed along the C(4)−C(7) direction. For example, the dihedral angle between the planes defined by the atoms C(3)−C(4)−C(5) and C(6)−C(7)−C(8) is 52° in **8a** and 99° in **8b**. The ^{1}H NMR spectrum of **8** in solution shows only two C_5H_5 resonances: 4.11 and 4.26 ppm, indicating that there is only a single structural isomer present in solution or, if both isomers are present, then they are rapidly interconverting on the NMR time scale at 25 °C.

The differential pulse (DP) voltammograms of compounds **4** and **5** show two very closely spaced, poorly resolved, one-electron oxidations for the ferrocenyl groups at $E = +0.50$ V and $+0.55$ V vs Ag/AgCl, $\Delta E_p = 0.05$ V and $E = +0.49$ V and $+0.51$ V (shoulder) vs Ag/AgCl, $\Delta E_p = 0.02$ V, respectively. By contrast, compound **6** shows two resolved one-electron oxidations for the ferrocenyl groups at $E = +0.38$ V and $+0.52$ V vs Ag/AgCl, $\Delta E_p = 0.14$ V. The redox processes of compound **7** were irreversible oxidations and were not studied further. The redox properties of the ferrocenyl groups of **8** are very similar to those of **4** and **5**, showing two very closely spaced, poorly resolved one-electron oxidations for the ferrocenyl groups at $E = +0.47$ V (shoulder) and $+0.50$ V, $\Delta E_p = 0.03$ V.

Discussion

As shown by the structures of **4** and **5**, the coordination of **3** to triosmium clusters is typical of that of simple alkynes[8b] and also that of 1,4-bis(ferrocenyl)butadiyne as found previously in compound **B**.[3] There are two different types of alkyne groupings in **3**, the inner pair and the outer pair, and the cluster can, in principle, become attached to either type. In fact, the cluster attaches to both, the outer in **4** and inner in **5**. On the basis of the isolated yield the preference for coordination at the inner alkyne site is 6 times greater than that for the outer alkyne site. This result can probably be explained by simple steric effects. The outer alkyne group is less accessible than the inner because of the proximity of the bulky ferrocenyl group.

The coordination of the alkyne groups of **3** to the open cluster in **6** is similar to that observed in the compound **A**[3] and similar to that observed for cis-dimetalated olefins.[12] The bonding in **6** could be viewed as two adjacent cis-dimetalated olefins **D** or as a butatrienyl dianion coordinated to an $Os_3(CO)_{11}$ dication, **E**, R = −C≡C−C≡C−Fc. The latter description would better

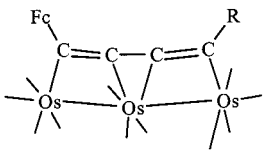

D

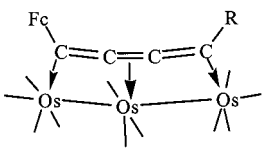

E

explain the observed shortening of the C−C bond between the two original alkyne groups. Interestingly, the difference between the redox potentials of the two ferrocenyl groups in **6** is quite significant, 140 mV, whereas in the free molecule no difference could be detected. This seems to suggest that there may be significant electrocommunication between the two ferrocenyl groups as previously demonstrated for compound **A**. However unlike **A**, where the two ferrocenyl groups are equivalent, the ferrocenyl groups in **6** are inequivalent, and this will contribute to the observed difference in their electrode potentials. The question is, how much will this inequivalence contribute to the difference in the electrode potentials? This of course cannot be measured directly; however we believe that it would be inappropriate to assume that all the observed potential difference is due solely to inequivalence for the following reason. In this study we have prepared three other osmium cluster complexes, **4**, **5**, and **8**, that can serve as models for estimating the differences in electrode potentials that might be produced by simple inequivalence. For all three of these compounds the difference in the ferrocenyl electrode potentials is no greater than 50 mV. Thus, we would argue that the very large potential difference found in **6** would imply that factors other than inequivalence are operative, and in view of the observations made previously for compound **A**, we believe that electrocommunication is not only a likely explanation for the difference in potentials but is also significant in amount.

The formation of compound **7** can be viewed as the addition of a second triosmium cluster to **6**. Indeed, we also synthesized **7** by the reaction of **6** with **1**. In the process a CO ligand from the added cluster was coupled to the tetrayne chain to form a five-membered heterocyclic ring that is linked to the new cluster via a terminal carbene center. The coupling of CO to alkynes has been used to prepare a wide range of new organic compounds;[13] however, the coupling of CO to polyynes has been little explored. This would seem to be an area of great potential for the synthesis of new organic molecules. Compound **7** exhibited no well-defined redox behavior, but it does have low-energy UV−vis absorptions that are typical of ferrocenyl carbocations.[11] Inspection of the structure of **7** shows that the carbon atom C(1), which contains a ferrocenyl substituent, is trivalent and planar. We believe that this site has considerable carbocation character, as indicated by the zwitterionic structure as shown in Scheme 1.

The formation of **8** from **5** plus **2** is simply the result of the addition of a second triangular triosmium cluster to one of the uncoordinated alkyne groupings of the ligand **3** in **5**. Interestingly, the closely spaced redox potentials of the ferrocenyl groups in each of **4**, **5**, and **8** suggest that there is very little electrocommunication between them. A similar result was found for the triosmium complex of 1,4-bis(ferrocenyl)butadiyne. This can be explained by the fact that the coordination of the alkyne groups to the clusters in **4**, **5**, and **8** involves both π-bonds of the coordinated C−C triple bond. If the electrocommunication is based on the π-orbital pathway,[2a] then the involvement of these orbitals in bonding to the

(12) Burke, M. R.; Takats, J. *J. Organomet. Chem.* **1986**, *302*, C25. (b) Dickson, R. S.; Johnson, S. H.; Kirsch, H. P.; Lloyd, D. J. *Acta Crystallogr.* **1977**, *B33*, 2057. (c) Clemens, J.; Green, M.; Kuo, M.-C.; Fritchie, C. J.; Mague, J. T.; Stone, F. G. A. *Chem. Commun.* **1972**, 53. (d) Davidson, J. L.; Harrison, W.; Sharp, D. W. A.; Sim, G. A. *J. Organomet. Chem.* **1972**, *46*, C47. (e) Koie, Y.; Shinoda, S.; Saito, J.; Fitzgerald, B. J.; Pierpont, C. *Inorg. Chem.* **1990**, *9*, 2350.

(13) Shore, N. E. *Chem. Rev.* **1988**, *88*, 1081. (b) Casalnuovo, J. A.; Shore, N. E. In *Modern Acetylene Chemistry*; Stang, P. J., Diederich, F., Eds.; VCH: Weinheim, 1995; Chapter 5.

metal atoms would inhibit the electrocommunication as observed. By contrast, in **6** the redox potentials of the ferrocenyl groups are significantly different. This is attributed to enhanced electrocommunication provided by greater interactions through the π-orbital network in the ligand **3** produced by the coordination to the metal atoms.

Acknowledgment. This work was supported by a Research Investment award from the University of South Carolina and the USC NanoCenter. We thank Mr. Burjor Captain for growing the crystal of **5**. Also we thank Professor Thomas Albright for helpful discussions about the bonding.

Supporting Information Available: CIF tables for the structural analyses of **4**, **5**, **6**, **7**, **8a**, and **8b**. This material is available free of charge via the Internet at http://pubs.acs.org.

OM0104060